Annual integral solar proton fluences since 1984: new reconstruction from GOES data

O. Raukunen[1,2] (oajrau@utu.fi), I. Usoskin[3], S. Koldobskiy[3], G. Kovaltsov[3], and R. Vainio[1]

[1]University of Turku, Finland

[2]Aboa Space Research Oy, Turku, Finland

[3]University of Oulu, Finland

Astronomy & Astrophysics

Home ▸ Forthcoming articles

Free Access

Annual integral solar proton fluences for 1984-2019

O. Raukunen, I. Usoskin, S. Koldobskiy, G. Kovaltsov, R. Vainio

A&A, Forthcoming article

Received: 08 April 2022 / Accepted: 17 June 2022

DOI: https://doi.org/10.1051/0004-6361/202243736

PDF (2.667 MB)

Data availability and data selection

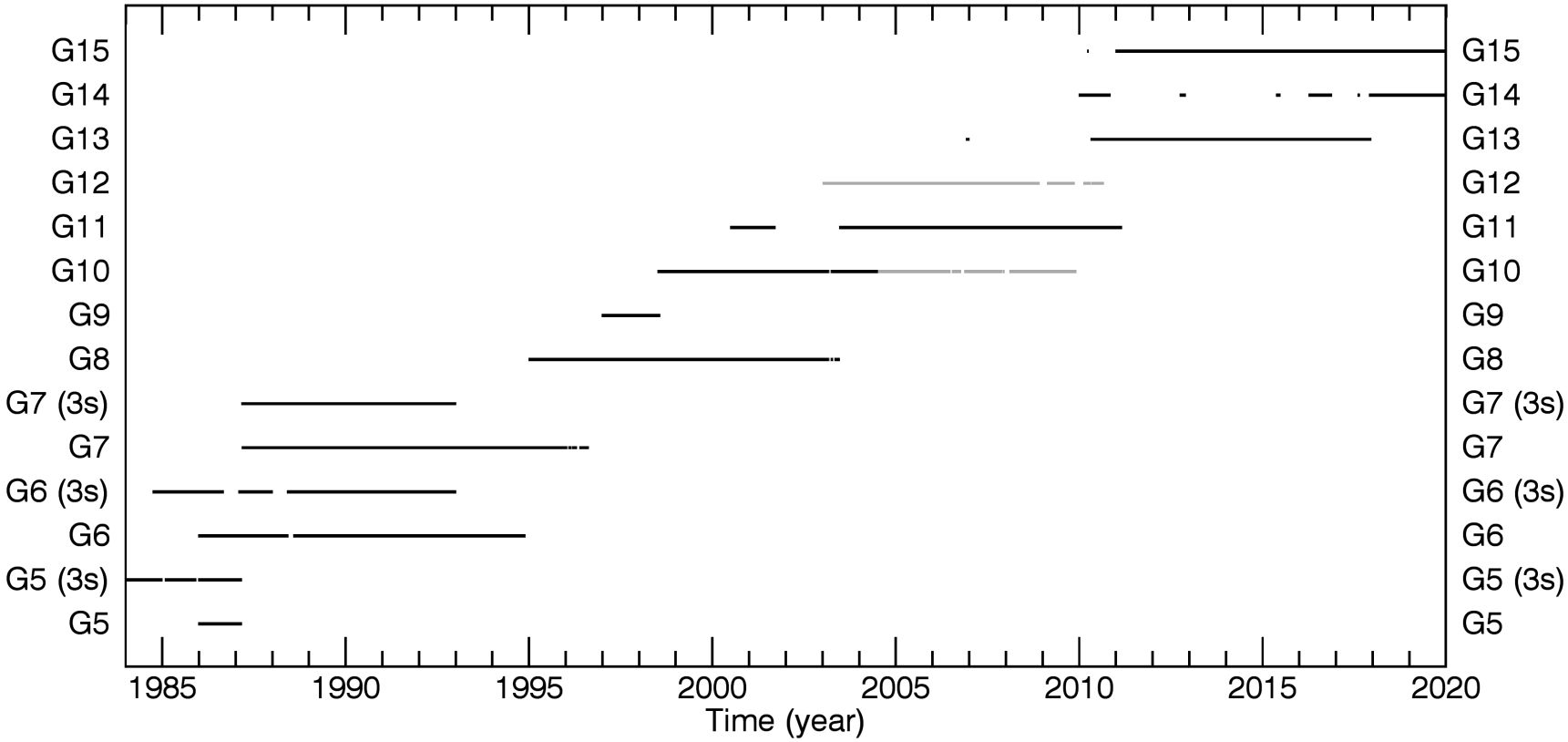

- Grey lines show times when measurements from the high energy channels P6 and P7 are not available.
- We used 5-min CSV-files from satdat.ngdc.noaa.gov
- For GOES 5 – 7 revised "3s" datasets were also considered.
- Since neither the corrected nor the integral fluxes are provided in the 3s-data, we chose to base our study on the "raw", or uncorrected, fluxes
- In case of GOES-13–15 we used the orientation flag datafiles to select fluxes observed by the westward-facing EPEAD

We identified and removed dropouts, spikes and periods of suspicious values between few hours and few days.

This operation is especially important for "noisy" GOES 5 – GOES 7.

Comparisons between different datasets

After cleaning all the individual datasets, we performed a comparison between each two overlapping differential datasets.

We quantified the agreement between the datasets by means of linear relationships between the measured fluxes f_x and f_y:

$$f_y = a + b\, f_x$$

Parameters a and b were calculated with the least absolute deviation (LAD) method and their errors estimated with the bootstrap method.

Satellite		P2		P3		P4		P5		P6		P7	
x	y	b	σ_b	b	σ_b	b	σ_b	b	σ_b	b	σ_b	b	σ_b
G05	G05 (3s)	1.000	0.000	1.000	0.000	1.000	0.000	1.000	0.000	1.000	0.000	0.999	0.000
G05	G06	1.052	0.004	0.724	0.003	0.149	0.001	0.889	0.004	1.017	0.001	1.017	0.001
G05	G06 (3s)	1.054	0.004	0.725	0.003	0.149	0.001	0.893	0.002	1.014	0.000	1.010	0.001
G05 (3s)	G06	1.053	0.004	0.723	0.003	0.149	0.001	0.886	0.003	1.017	0.001	1.018	0.000

Satellite		P2		P3		P4		P5		P6		P7	
x	y	a	σ_a	a	σ_a	a	σ_a	a	σ_a	a	σ_a	a	σ_a
G05	G05 (3s)	0.000	0.000	−0.000	0.000	−0.000	0.000	−0.000	0.000	0.000	0.000	0.000	0.000
G05	G06	−0.020	0.006	−0.000	0.008	0.046	0.001	0.002	0.000	0.000	0.000	0.000	0.000
G05	G06 (3s)	−0.026	0.008	−0.001	0.008	0.045	0.001	0.001	0.000	0.000	0.000	0.000	0.000
G05 (3s)	G06	−0.023	0.007	0.008	0.008	0.046	0.001	0.002	0.000	0.000	0.000	0.000	0.000
G05 (3s)	G06 (3s)	−0.043	0.005	0.020	0.005	0.071	0.002	0.002	0.000	0.000	0.000	0.000	0.000

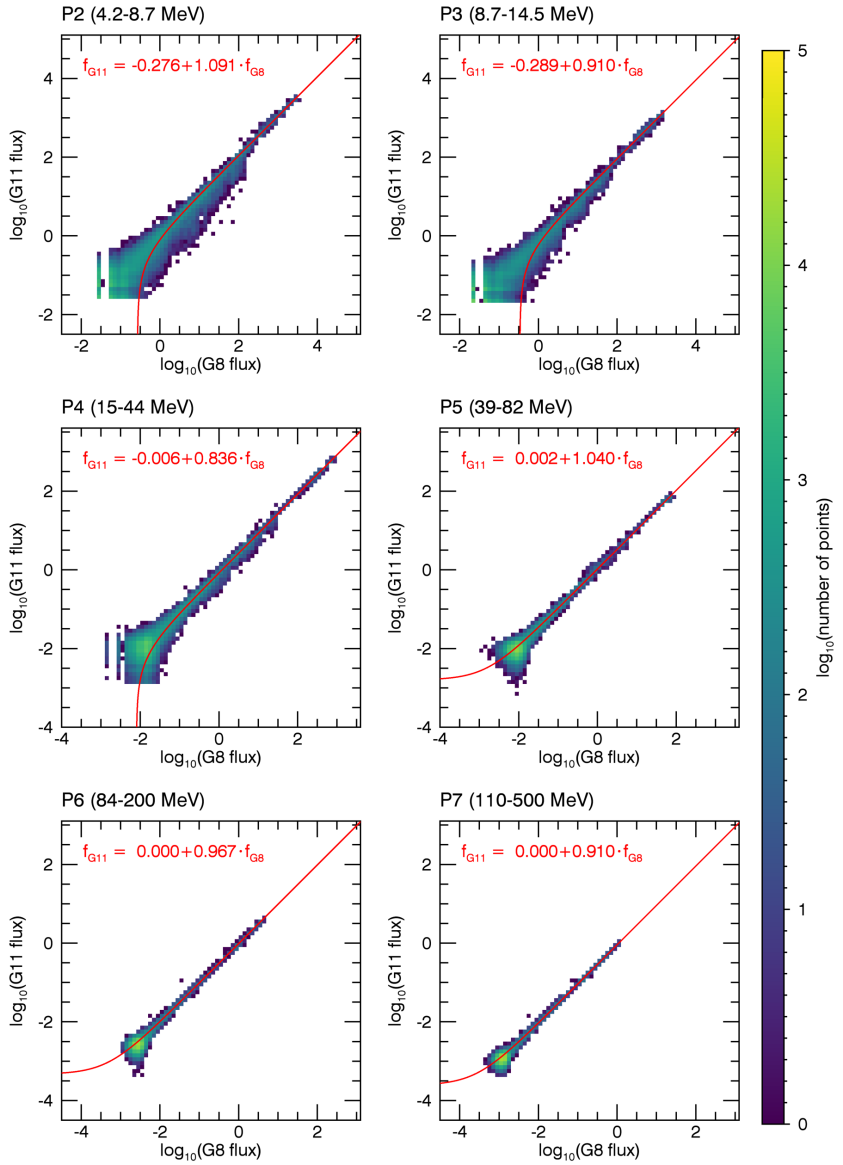

Comparison between different datasets

In general, good agreement for GOES 5 - 7 and 8 - 15, but noticeable difference for GOES-7 and GOES-8 (channels P4 – P7), which we assume is caused by different geometric factor in the data processing of the first GOES generation.

We decided to correct GOES 5 - 7 because there is no obvious disagreement between the later GOES generations and their data are well studied.

To do this, we reconstructed the GdE values using the 3s-data, which include the number of samples for each channel.

Channel	Energy range[a] (MeV)	Eff. energy (MeV)	*GdE* 1st gen. data processing[b] (cm^2 sr MeV)	*GdE* This study[a] (cm^2 sr MeV)
P2	4.2–8.7	5.916	0.252	0.252
P3	8.7–14.5	11.11	0.325	0.325
P4	15–44	24.53	6.09	4.64
P5	39–82	55.29	20.0	15.5
P6	84–200	125.7	136.0	90.0
P7	110–500	214.9	891.0	300.0

After correcting the geometric factor for the GOES 5 - 7 fluxes, the majority of the differences between the observations are within 30%.

SEP integral fluxes

In order to calculate the integral proton fluxes of solar origin, we subtract the GCR background from the differential fluxes.

The background flux is defined as the smallest daily flux for each
10-day period, calculated separately for each channel of each EPS/EPEAD instrument.

In order to prevent long-duration SEP events or lingering data problems affecting the background, each background value greater than 1.5 times or smaller than 0.5 times the mean of three previous
background values is replaced with the mean.

To improve the uniformity of the data, we select GOES-8 as the baseline and correct each differential channel of the other selected data sources to the same level using the intercalibration results. GOES-8 is selected because of its coverage as well as its data quality.

Sources of data used to create a dataset covering the time period from 1984 to 2019

1984-01-01 – 1984-12-31	GOES-5 (3s)
1985-01-01 – 1985-01-31	GOES-6 (3s)
1985-02-01 – 1985-11-30	GOES-5 (3s)
1985-12-01 – 1985-12-31	GOES-6 (3s)
1986-01-01 – 1986-12-31	GOES-5 (3s)
1987-01-01 – 1987-02-28	GOES-7
1987-03-01 – 1987-03-31	GOES-6 (3s)
1987-04-01 – 1991-10-14	GOES-7
1991-10-15 – 1991-10-31	GOES-6 (3s)
1991-11-01 – 1994-12-31	GOES-7
1995-01-01 – 2003-03-31	GOES-8
2003-04-01 – 2003-05-14	GOES-10
2003-05-15 – 2003-06-14	GOES-8
2003-06-15 – 2003-06-30	GOES-10
2003-07-01 – 2010-12-31	GOES-11
2011-01-01 – 2019-12-31	GOES-15

SEP integral fluxes II

The integral fluxes were calculated using background-subtracted, 1-hour averaged differential fluxes, assuming a piecewise power-law between the "effective" channel energies E_{ch}, which were defined as

$$E_{ch} = \left(\frac{(-\gamma + 1)(E_h - E_l)}{E_h^{-\gamma+1} - E_l^{-\gamma+1}} \right)^{\frac{1}{\gamma}}$$

where E_l and E_h are the channel's lower and upper energy limits, and γ is the exponent of the power law spectrum. Instead of the commonly used γ = 2, which results in the geometric mean of the channel limits, we used γ = 3, which describes an SEP event spectrum more realistically above ~10 MeV energies.

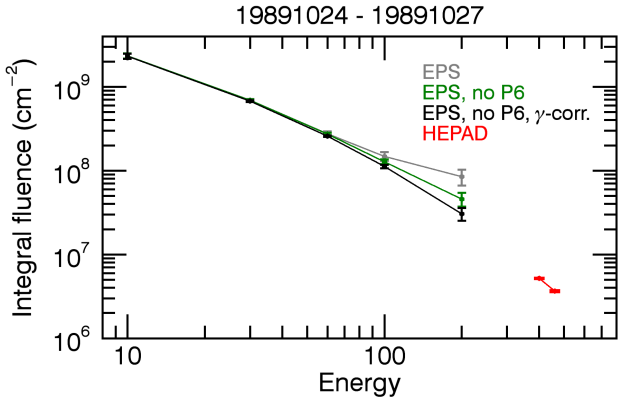

Channels P4 and P6 were not used in the integral flux calculation. GOES/HEPAD data was used to derive a spectral correction for the integral flux above P7 to avoid overestimation in the highest energies.

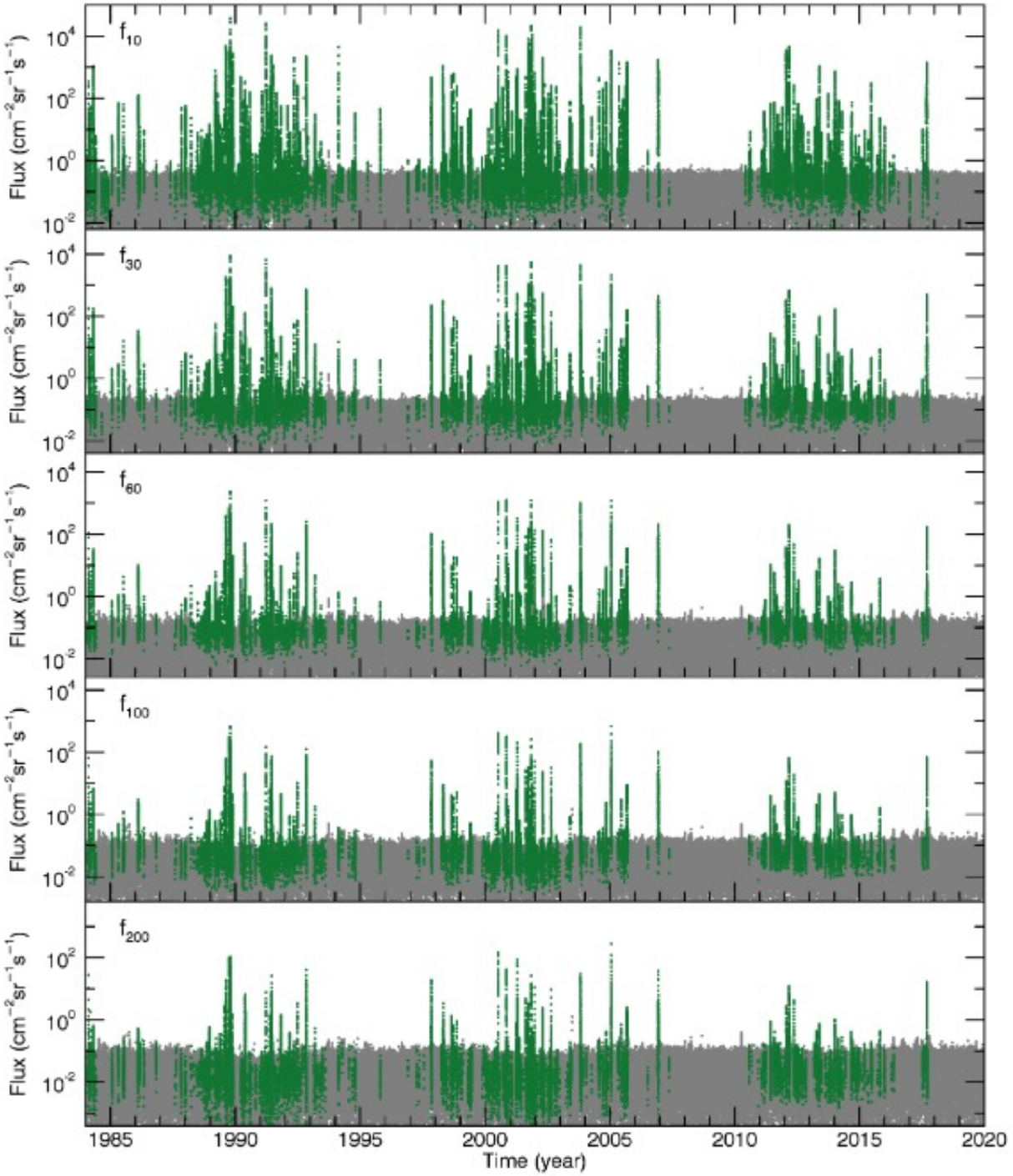

Results: SEP integral fluxes

Integral flux time series for the time period from 1984 to 2019 for f_{10}, f_{30}, f_{60}, f_{100} and f_{200}, respectively from top to bottom. Event periods are shown in green.

Event period selection:

- The non-background-subtracted 1-hour differential flux has to exceed the background by more than two times the statistical error of the background for at least six consecutive hours simultaneously in the channels above and below the integral energy;

– The maximum background-subtracted 1-hour differential flux in the P2 channel has to exceed 0.1 $cm^{-2}sr^{-1}s^{-1}MeV^{-1}$ during the event;

– At least 50% of the event is observed (i.e., not interpolated data gaps)

– Any period fulfilling the three previous event conditions at threshold energy E_i is also marked as an event at all integral energies below E_i

Results: comparison with other reconstructions

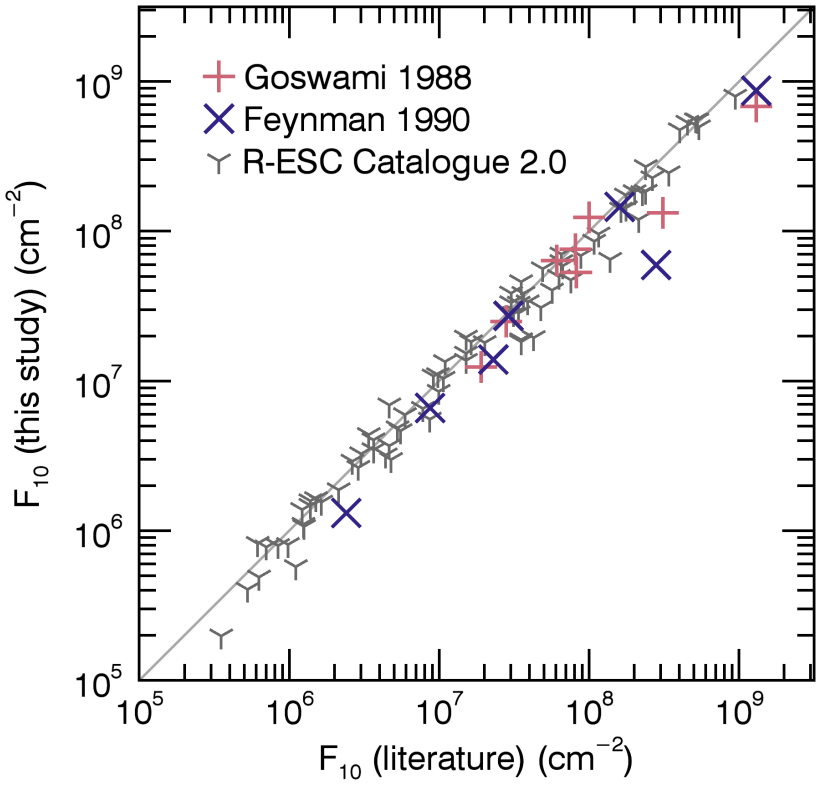

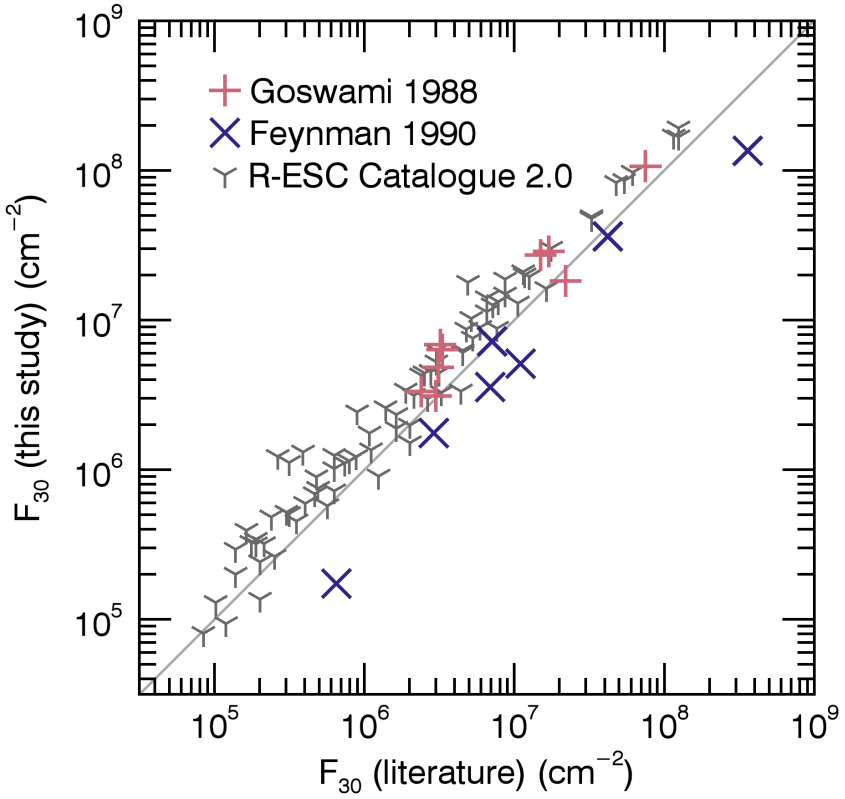

Goswami 1988 and **Feynman 1990**: comparison for largest events 1984–1986

R-ESC catalogue 2.0: comparison for 1997 – 2017

Mostly, the results are in good agreement, however, both Goswami et al. (1988) and Feynman et al. (1990) report higher fluences for F_{10}, but for F_{30}, our results tend to be higher than those in Goswami et al. (1988) and the R-ESC catalogue.

The difference can be up to several times, but only for few events.

Results: Annual fluences for period 1984 – 2019

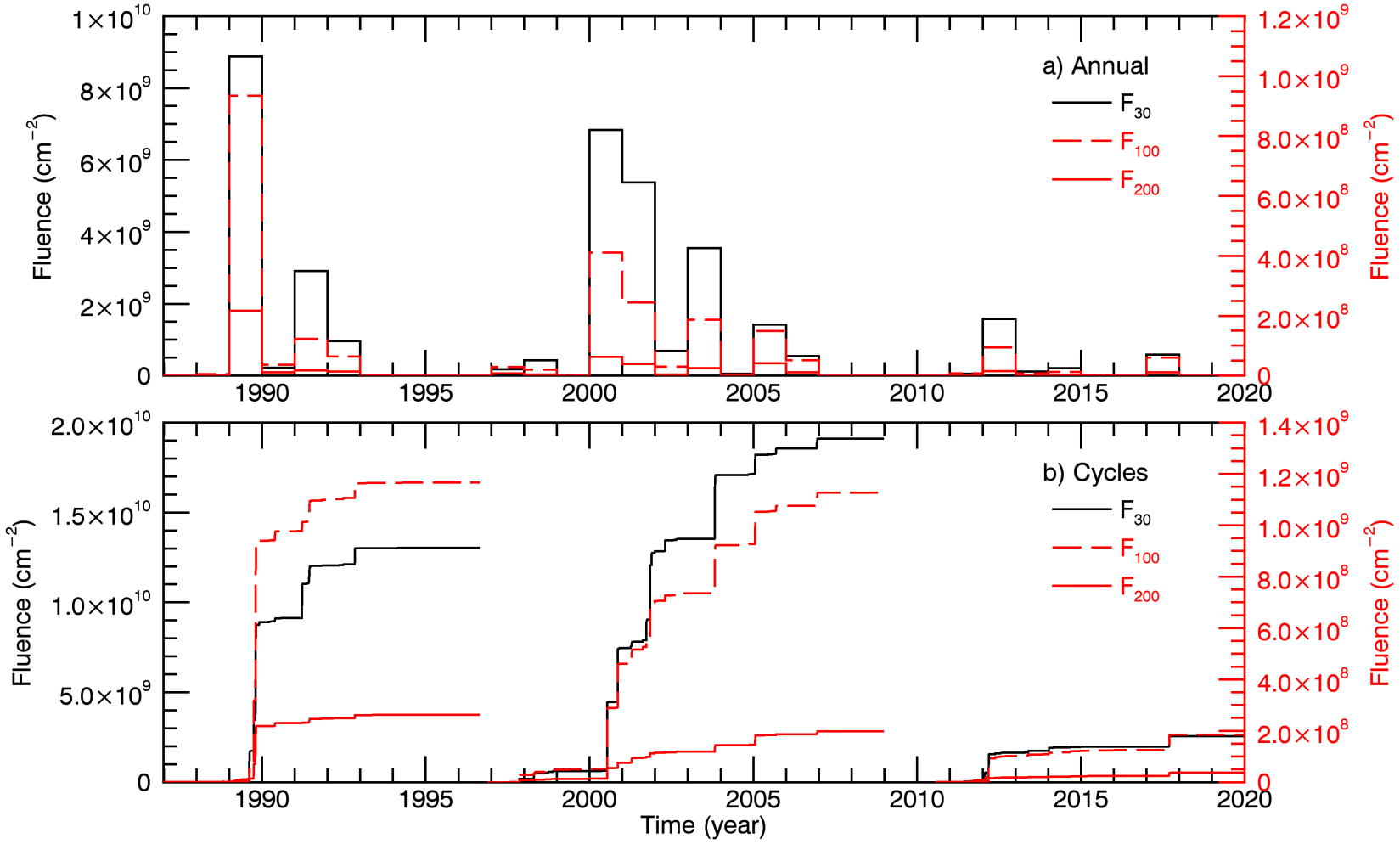

Annual solar proton fluences and their error estimates for years 1984–2019

Year	F_{10}	$\sigma_{F_{10}}$	F_{30}	$\sigma_{F_{30}}$	F_{60}	$\sigma_{F_{60}}$
1984	$1.05 \cdot 10^{9}$	$2.53 \cdot 10^{7}$	$1.80 \cdot 10^{8}$	$4.85 \cdot 10^{6}$	$4.30 \cdot 10^{7}$	$8.19 \cdot 10^{5}$
1985	$8.31 \cdot 10^{7}$	$2.79 \cdot 10^{6}$	$1.22 \cdot 10^{7}$	$8.81 \cdot 10^{5}$	$4.23 \cdot 10^{6}$	$3.49 \cdot 10^{5}$
1986	$2.69 \cdot 10^{8}$	$6.77 \cdot 10^{6}$	$4.88 \cdot 10^{7}$	$1.19 \cdot 10^{6}$	$1.33 \cdot 10^{7}$	$5.71 \cdot 10^{5}$
1987	$3.01 \cdot 10^{7}$	$2.14 \cdot 10^{6}$	$2.35 \cdot 10^{6}$	$6.82 \cdot 10^{5}$	$6.96 \cdot 10^{5}$	$3.54 \cdot 10^{5}$
1988	$1.44 \cdot 10^{8}$	$7.71 \cdot 10^{6}$	$2.77 \cdot 10^{7}$	$1.73 \cdot 10^{6}$	$9.97 \cdot 10^{6}$	$8.14 \cdot 10^{5}$
1989	$3.23 \cdot 10^{10}$	$8.57 \cdot 10^{8}$	$8.88 \cdot 10^{9}$	$1.66 \cdot 10^{8}$	$2.72 \cdot 10^{9}$	$4.23 \cdot 10^{6}$
1990	$1.14 \cdot 10^{9}$	$3.26 \cdot 10^{7}$	$2.18 \cdot 10^{8}$	$6.65 \cdot 10^{6}$	$8.05 \cdot 10^{7}$	$1.04 \cdot 10^{6}$
1991	$1.18 \cdot 10^{10}$	$4.71 \cdot 10^{8}$	$2.91 \cdot 10^{9}$	$1.53 \cdot 10^{8}$	$6.02 \cdot 10^{8}$	$3.65 \cdot 10^{6}$
1992	$3.97 \cdot 10^{9}$	$3.75 \cdot 10^{8}$	$9.66 \cdot 10^{8}$	$3.76 \cdot 10^{7}$	$2.35 \cdot 10^{8}$	$2.13 \cdot 10^{6}$
1993	$4.10 \cdot 10^{7}$	$2.84 \cdot 10^{6}$	$1.02 \cdot 10^{7}$	$1.20 \cdot 10^{6}$	$3.28 \cdot 10^{6}$	$4.24 \cdot 10^{5}$
1994	$6.76 \cdot 10^{8}$	$1.19 \cdot 10^{8}$	$7.24 \cdot 10^{6}$	$9.51 \cdot 10^{5}$	$1.75 \cdot 10^{6}$	$3.74 \cdot 10^{5}$
1995	$1.90 \cdot 10^{7}$	$1.56 \cdot 10^{6}$	$1.57 \cdot 10^{6}$	$3.28 \cdot 10^{5}$	$2.72 \cdot 10^{5}$	$2.47 \cdot 10^{5}$
1996	$4.82 \cdot 10^{5}$	$4.85 \cdot 10^{5}$	$3.96 \cdot 10^{4}$	$1.90 \cdot 10^{5}$	$1.67 \cdot 10^{4}$	$9.02 \cdot 10^{4}$
1997	$5.11 \cdot 10^{8}$	$1.16 \cdot 10^{7}$	$1.79 \cdot 10^{8}$	$3.40 \cdot 10^{6}$	$6.86 \cdot 10^{7}$	$6.20 \cdot 10^{5}$
1998	$2.21 \cdot 10^{9}$	$3.08 \cdot 10^{7}$	$4.32 \cdot 10^{8}$	$4.00 \cdot 10^{6}$	$8.69 \cdot 10^{7}$	$2.03 \cdot 10^{6}$
1999	$1.25 \cdot 10^{8}$	$8.42 \cdot 10^{6}$	$1.38 \cdot 10^{7}$	$1.11 \cdot 10^{6}$	$3.98 \cdot 10^{6}$	$6.01 \cdot 10^{5}$
2000	$2.28 \cdot 10^{10}$	$7.94 \cdot 10^{7}$	$6.84 \cdot 10^{9}$	$2.59 \cdot 10^{7}$	$1.72 \cdot 10^{9}$	$3.29 \cdot 10^{6}$
2001	$2.61 \cdot 10^{10}$	$1.04 \cdot 10^{8}$	$5.38 \cdot 10^{9}$	$1.14 \cdot 10^{7}$	$1.11 \cdot 10^{9}$	$4.00 \cdot 10^{6}$
2002	$3.37 \cdot 10^{9}$	$3.89 \cdot 10^{7}$	$6.89 \cdot 10^{8}$	$6.18 \cdot 10^{6}$	$1.44 \cdot 10^{8}$	$1.63 \cdot 10^{6}$
2003	$1.37 \cdot 10^{10}$	$5.70 \cdot 10^{8}$	$3.55 \cdot 10^{9}$	$6.15 \cdot 10^{7}$	$8.26 \cdot 10^{8}$	$4.65 \cdot 10^{6}$
2004	$7.23 \cdot 10^{8}$	$1.66 \cdot 10^{7}$	$5.73 \cdot 10^{7}$	$1.45 \cdot 10^{6}$	$1.14 \cdot 10^{7}$	$7.82 \cdot 10^{5}$
2005	$6.19 \cdot 10^{9}$	$1.22 \cdot 10^{8}$	$1.42 \cdot 10^{9}$	$1.70 \cdot 10^{7}$	$4.11 \cdot 10^{8}$	$3.29 \cdot 10^{6}$
2006	$2.43 \cdot 10^{9}$	$6.26 \cdot 10^{7}$	$5.44 \cdot 10^{8}$	$6.19 \cdot 10^{6}$	$1.55 \cdot 10^{8}$	$1.45 \cdot 10^{6}$

...

...

Cumulative probability density functions

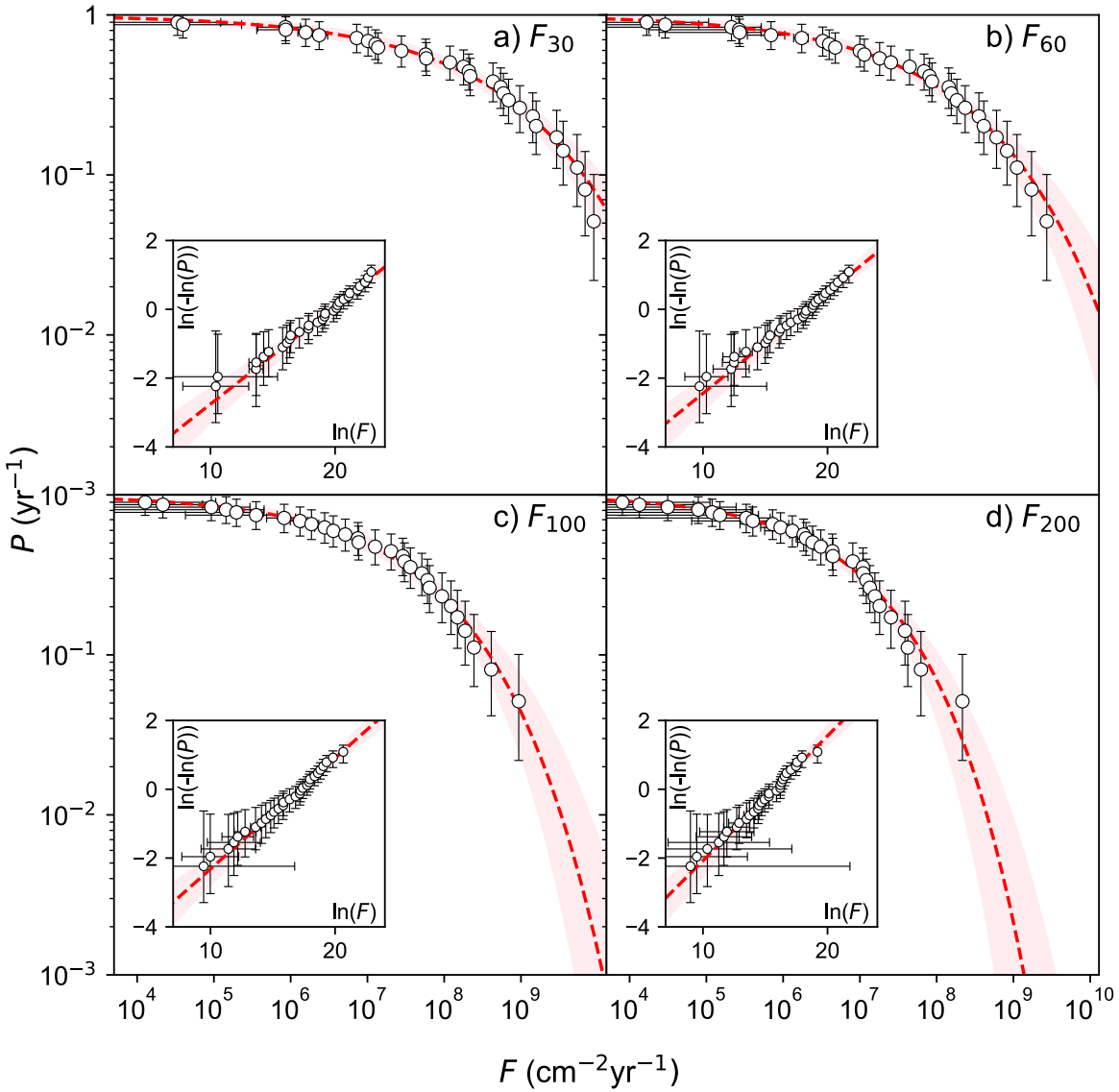

CCDF shows the probability that the annual fluence will exceed some value for randomly chosen year.

This probability can be described very well with Weibull function:

$$P = \exp\left(-(F/\lambda)^{\kappa}\right)$$

Parameter	F_{30}	F_{60}	F_{100}	F_{200}
κ	$0.29^{+0.05}_{-0.04}$	$0.29^{+0.05}_{-0.05}$	$0.32^{+0.06}_{-0.05}$	$0.36^{+0.07}_{-0.06}$
λ (cm^{-2})	$\left(3.50^{+1.45}_{-1.01}\right)\cdot 10^{8}$	$\left(9.18^{+3.68}_{-2.59}\right)\cdot 10^{7}$	$\left(2.92^{+1.03}_{-0.77}\right)\cdot 10^{7}$	$\left(6.73^{+2.06}_{-1.56}\right)\cdot 10^{6}$

Conclusions

- We have reconstructed the annual SEP fluences in five energy ranges, viz. above 10, 30, 60, 100 and 200 MeV for the period from 1984–2019, using the revisited calibration of in-situ data obtained on-board GOES-family spacecraft.
- It is found that the SEP accumulated fluences during solar cycle 24 were significantly (a factor of 5–7) smaller than during the previous cycles 22 and 23.
- The solar-cycle fluence is accumulated mostly during strong SEP events, e.g., 70–90 % of the fluence for cycle 22 was accumulated during a series of strong SEP events in the Autumn of 1989.
- CCDFs of the annual fluences depict a fast roll off for high values of the fluences and are nearly perfectly described by the Weibull- distribution shape.
- Annual fluences, as well as time series of integral SEP fluxes f_{10}, f_{30}, f_{60}, f_{100} and f_{200} at 1-hour resolution, will be provided at the CDS.